Application of terrestrial 3D laser scanner in quantification of the riverbank erosion and deposition

M.H. Nasermoaddeli & E. Pasche
Institute of river and coastal engineering, Technical university Hamburg-Harburg, Hamburg, Germany

Abstract
Previous measurements of the riverbank erosion have been based often on sparse spatial and temporal data-sets with large uncertainties. Recently, the application of airborne laser scanning has removed this shortcoming in large scale areas. However, for detailed study of the erosion process of a small river reach, the mentioned method is not efficient. This gap can be closed by terrestrial laser scanning, which has been applied in the current work.
A small reach of a riverbank was scanned over two flooding periods. The bathymetry of wet area was measured by a shallow-water echo-sounder. An integrated DTM model was generated for the riverbank and bank-toe using a special method. The DTM generation for very steep and often negative bank slopes required a coordinate transformation by 90°.
This method reduces the possibility of unscanned areas due to the shadowing effect of the roughness elements and negative bank slopes. The spatial distribution of erosion and deposition areas and the corresponding volumes were determined by subtracting the successive integrated DTMs and were analysed in respect to the flood hydrograph to demonstrate the morphological processes in the riverbank along the river bend. A conceptual model of the riverbank erosion was proposed for fine sandy riverbanks.

Keywords: Terrestrial 3D laser scanner, Riverbank retreat, Erosion and deposition volume, Shallow-water echo-sounder, RTK-GPS.

1 INTRODUCTION

Riverbank erosion is one of the most important processes in lateral migration of the river channel. Bank erosion claims every year fertile agricultural lands in the margin of the rivers all around the world and contributes to the suspended sediment load (often contaminated with agricultural nutrients and pesticides) in the rivers. Study of the riverbank erosion is a key issue in meander restoration programs, which are essential for rehabilitation of aquatic life.
Field measurements provide an important insight into the processes involved in riverbank erosion. Most of the field measurement techniques applied in the previous studies were unable to quantify small-scale changes in the riverbank, which trigger large-scale morphological changes. Lawer (1993) made a comprehensive review and discussion of these measurement techniques for the study of the bank erosion and divided them into seven categories depending on the temporal and spatial scale of the study, among which, erosion pins, PEEP (Photo Electric Erosion Pins) and terrestrial photogrammetry applied to short time scale. The mentioned methods suffer from either or both spatial and temporal resolution and are labour-intensive in pre- and post processing phases.
Technical advances in hardware applied for surveying and software for post-processing

huge amount of data, paved the way for acquiring more accurate data with higher resolution. High precision total station surveying (Fuller et al 2003), Real-Time Kinematics Global Positioning System(RTK-GPS) (Brasington et al,2000; Mitasova et al ,2002) and airborne LiDAR (Light Detection and Ranging) techniques (Thoma et al. 2001,2005) have been applied recently in the study of river and coastal morphology.

Total station offers a very high accuracy but relatively low spatial resolution. In the case of very steep or vertical riverbanks, it is also not applicable. The same limitations hold for GPS in addition to lower accuracy. Airborne LiDAR systems provide relative high accuracy and high spatial resolution. However, it is feasible for the study of large areas with limited temporal resolution. Application limitations of the mentioned methods are discussed in Heritage and Hetherington (2007) and Milan et al (2007).

With recent developments in LiDAR technology, very high spatial resolution and accuracy is attainable by terrestrial laser scanning, with much higher temporal resolution than its airborne version. This technique has been often applied in industry, piping, architecture, archaeology and has found its way into geology and landslide studies (Bitelli et al,2004), in-stream habitat quantification (Large and Heritage,2007), study of gravel-bed forms (Entwistle et al,2007) and assessment of erosion and deposition in proglacial rivers (Milan et al,2007).

Detailed study of erosion and deposition processes of the natural riverbanks with complex surface requires a very high spatial resolution to reduce the possibility of un-scanned areas due to the shadowing effect of roughness elements and overhanging zones.

This paper reports such an application of terrestrial laser scanning technique to investigate the riverbank erosion and deposition mechanism. This technique was combined with RTK-GPS integrated with a shallow-water single-beam echo-sounder for the measurement of the bed surface under water surface (bathymetry), where laser scanner is not applicable.

2 STUDY SITE

The study was carried out on the river Hardebek-Brokenlander Au, which discharges to the upper reach of the river Stoer near Neumuenster in north of Germany (figure1).

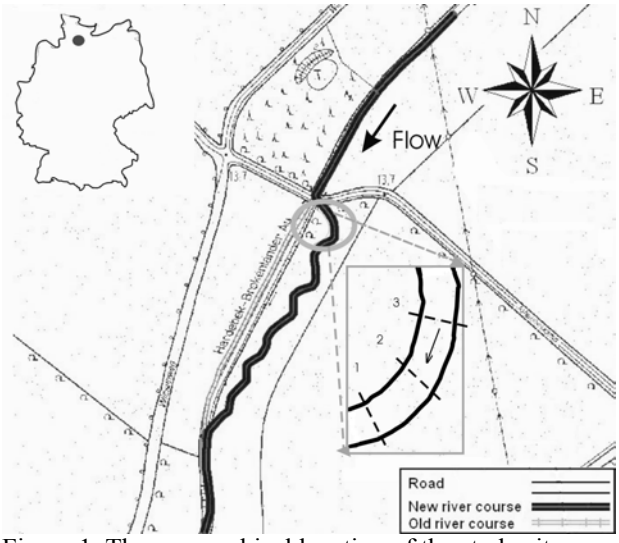

Figure 1. The geographical location of the study site .

It is a small shallow stream (table 1) of fine sandy bank with overlaying clay layer of 25 to 40 cm thickness covered with vegetation. The stream was formerly a straight canalised stream, which was then diverted to a new course to create a self-forming meandering stream for the purpose of meander restoration studies.

Table1. Hydraulic and morphological characteristics of the study reach of the river .

Flow Parameters	Measured in 2007
Discharge (m^3/s)	0.31-1.36
Mean velocity (m/s)	0.21-0.45
Bank full width (m)	5.3-9.0
Average water depth range (m)	0.28-1.0
Mean bed slope(%)	0.12
Riverbank properties (sand layer)	
D_{50} (mm)	0.2
$C_c=D_{30}^2/(D_{60}xD_{10})$	1.048
$C_u=D_{60}/D_{10}$	1.811
Meander Properties	
Radius of curvature (m)	16.40
Meander length (m)	50.44
Sinuosity	1.25

3 METHODLOGY

A severe eroding reach of the river bend(with vertical and negative slope) was selected for the study of riverbank erosion mechanism (figure 2). The study area covered over 13 m length of the outer bank of the river bend with 0.80 to 1.3m bank height. Scanning was achieved intermittently in two phases over flooding periods of October 2006 to April 2007 and October 2007 to December 2007 using Leica Cyrax HDS2500 3D laser scanner. Additional river bed bathymetry was achieved in the second phase by using RTK-DGPS system (Leica System 500-SR350) integrated with a single-beam echo-sounder (Fahrentholz BBES 700 kHz) to build later an integrated riverbank and bed elevation model. Flow depth was recorded continuously using differential pressure sensor upstream and downstream of the study site on the first phase.

Figure 2. The outer riverbank of the meander under study.

3.1 Laser scanner

The instrument works on the principle of "time of flight" measurement using a pulsed green visible (VIS) laser source (wave length of 532 nm, safety class II). The emission of the laser source is controlled by a servo motor-driven spinning plane mirror.
The single point accuracy of the instrument in the range between 1.5 and 50 m is 6 mm (position), 4mm (distance) and 0.003° (angle); and the accuracy of the modelled surface is 2 mm. The highest scan resolution is 0.25 mm point-to-point spacing (vertical and horizontal) in 50 m range. The vertical and horizontal measurement spacing can be defined independently. The instrument field of view is 40° x 40° (horizontal x vertical). The maximum application range of the instrument is 100 m.
The study area was scanned in two overlapping regions due to the instrument's small field of view. Six targets were placed in each region and scanned with extra dense resolution for later registration of two overlapping scans and merging in Cyclone® 4.0 (the post-processing object oriented software of the laser scanner). Each merged point cloud was geo-referenced in the mentioned software using surveyed coordinates of the targets by the total station Leica TCR705.
Surveying using laser scanner were achieved on 25 Oct. and 12 Dec. 2006, 5 and 30 Jan. 2007, 14 Feb. and 16 April 2007 , designated as first phase and once on 10 Dec. 2007, designated as the second phase. The later was accompanied by bathymetry measurement using a single-beam echo-sounder. The aim was integration of the high resolution laser scanning data with low resolution echo-sounder data for the study of bank-toe processes.
Flow discharge and water depth were recorded continuously from 5 Jan. 2007 till 16 April 2007. Flow discharge was monitored by a house-modified ADCP StreamPro® (RDI) for the purpose of long term measurement using velocity-index method. However, for improving the telemetry system, the device was out of service for the period from 5 Jan. 2007 to 13 Feb.2007.

3.2 Echo-sounder

In the second phase of the measurements, a shallow-water single-beam echo-sounder was applied for surveying the area under water, where laser scanner was not applicable. (20 July, 24 Oct. , and 10 Dec. 2007).
The device transmit a 700 KHz sound wave and measures the time of returned echo from the bed surface to the transducer in order to measure the depth and records them in 10 Hz with an accuracy of 1 cm.

The echo-sounder was integrated with the rover antenna of the RTK-DGPS system (with a maximum of 2 cm accuracy during the measurements) and mounted on a floating round Styrofoam to form the bathymetry measurement system. The whole system was then towed across and along the stream.

3.3 Pre-processing

All of the point clouds were cut by a defined three dimensional polygon as a bounding region, common to all scans, for the analysis of bank erosion and deposition. The bounding limit was dictated by different water stages at the time of scanning and the elevation of vegetated layer over top of the bank.

A Fortran program was written to filter the over-hanging grasses from the point clouds. The filter algorithm creates a vertical mesh over the bank surface and transforms the coordinates to a local cylindrical coordinate system with laser scanner as its origin. Then, it computes the average and standard deviation of radial distance of the points to the origin within each grid cell. The points within each grid cell with a standard deviation larger than a user specified threshold are deleted .

Having bounded and filtered the point clouds, surface models (TIN and DTM, depending on the software applied) were created out of each point cloud for the computation of erosion and deposition surfaces. However, the generated surface models in common available softwares, such as FlederMouse®, Surfer® , ArcView® and Sycode TerrainCad plug in for AutoCad®, were erroneous in the zones with vertical and negative slopes (figure 3), since the surface can not be folded in the vertical direction in generation of digital surface models.

While the Cyclone® 4.0 software was able to generate a complex 3D folded fine mesh, it could neither achieve surface difference computations between two meshes in the software nor export the mesh to be analysed in another software. Even if it would be the case, it would not be possible to create a difference surface with traditional methods, due to the local folded zones in the mesh surface.

A coordinate translation and rotation was achieved, as explained in the following, to remedy the mentioned problems.

a) Point cloud in original coordinate system

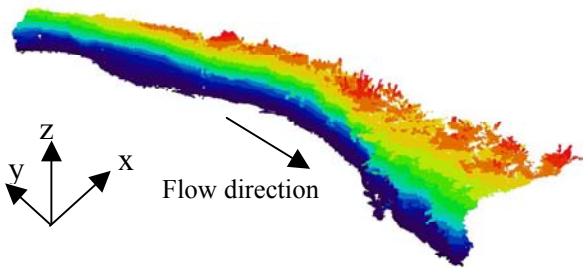

b) DTM model in original coordinate system.

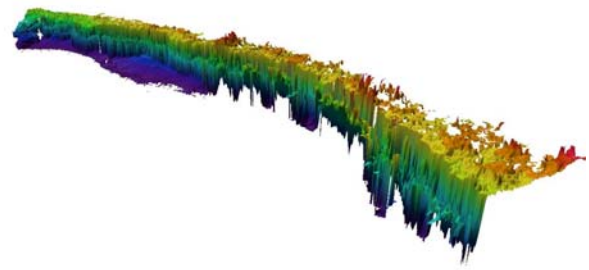

Figure 3. Error in generation of DTM of the riverbank in the vertical- and negative-slope regions of the riverbank in FlederMouse software.

The Gauss-Krueger coordinate system were translated to a local coordinate (with an scaling factor) and rotated about y axis 90° clock wise, so that the bank surface lay on the horizontal plane (y-z plane) with x axis directing down in negative direction of the former z axis. The DTM model was created in the new mentioned transformed coordinate system in FlederMouse® (figure 4-a). The coordinates were then rotated back for visualization purposes in graphical environment of the software (figure 4 –b).

The echo-sounder data was also first filtered to omit low accuracy (<4cm in position) GPS data as well as noise caused by floating objects and bed vegetation. The deleted points were then interpolated by triangulation method, which yielded in generation of DTM model.

In the case of the data of 24 Oct.2007, the high resolution laser scanner data of bank-toe were integrated to the low resolution irregularly spaced echo-sounder data and then a DTM model was generated for the integrated set of data.

a) DTM in rotated local coordinate system.

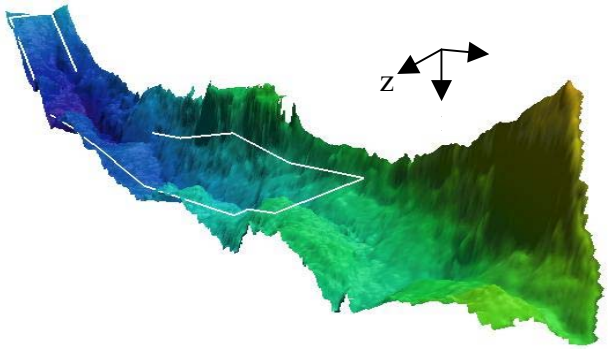

b) DTM viewing back in original direction of axes.

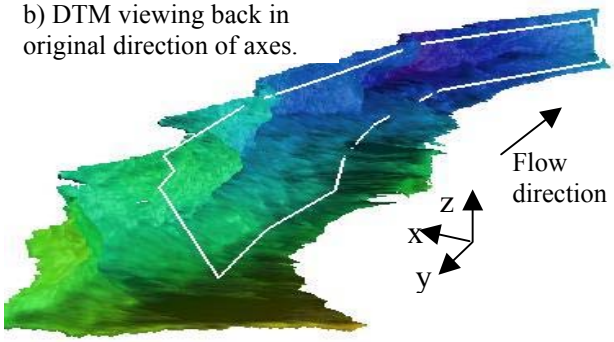

Figure 4. Generated DTM model of outer riverbank. The white polygon is the bounding limit.

4 ANALYSIS

After pre-processing the data as described above, the surface model of the scanned riverbank zone in the rotated coordinate were subtracted consecutively to obtain difference surfaces, which depicts erosion and deposition zones. In the following, the analysis of each phase of the measurements will be presented separately.

As it is seen from the flow hydrograph in figure(5), during 25 Oct. 2006, to 4 Jan. 2007, no flow measurements were achieved, therefore correlation of water stages with bank erosion was not possible for this period.

The first phase

For the analysis purposes, we have divided the bank surface in three vertical slices (I,II,III, meaning: upstream, middle and downstream part of the river bend) and in three layers (Top, Middle, Bottom). For example, (IIB) means the

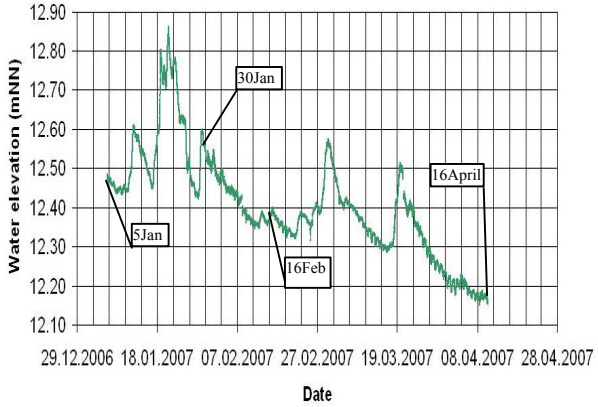

Figure 5. Hydrograph immediately downstream of the river bend.

zone locating in the middle slice and bottom layer and (III) means the whole third slice. Moreover, for each zone a representative cross section has been introduced to explain the riverbank retreat process better. The position of these cross sections are shown in figure 6.

a) Front view of the DTM surface of the riverbank.

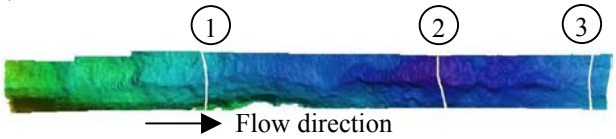

b) Longitudinal profiles along the outer river bend.

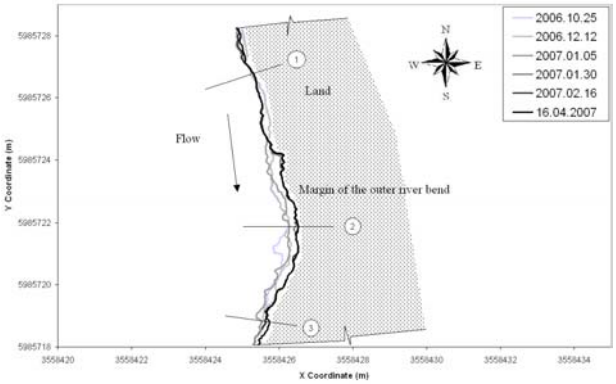

Figure 6. Position of the representative cross sections.

As it can be inferred from figure (7), during the period of 25 Oct. 2006 and 12 Dec. 2006, the middle layer(M) of the bank, especially in zones (II) and (III), has been severely eroded (undercutting by flow along the river bend), creating overhanging (positive depths in the legend) as well as bank failure (negative depths in legend) in layer (T). Moreover, there is little changes in the riverbank surface in zone(I), whereas riverbank and bank-toe erosion are moderate in zone(II) and intensive in zone(III)

due to increasing wall shear forces towards the exiting section of the river bend as a result of helical flow motion in the river bend.
The erosion volume within this period was -0,299 m^3 while deposition volume was 0.026 m^3 ,reflecting net erosion, which is given in table 2.
In the period of 12 Dec. 2006 and 5 Jan. 2007, bank-toe erosion combined by undercutting has played the role of triggering cantilever bank failure through increasing bank height and slope (often negative slope). The collapsed bank material has been mostly deposited on layers (B) and (M). Vegetation roots in top layer has allowed formation of the soil overhanging in a portion of the zone (IT).
An erosion volume of -0.088 m^3 and deposition volume of 0.442 m^3 were computed for this period. Other computed parameters are given in table 2.
In the period between 5 and 30 Jan. 2007, the highest flood event with multiple peaks has occurred (figure 5). The four highest peaks with water level ranging from 12.70 m and 12.86 m has occurred in a relatively short duration (2007.01.18,17:23 and 2007.01.22, 23:53), leaving a cutting zone at the same elevation interval at layer (M) all along the river bend. It can be concluded that the frequency of flood peaks may play an important role in the erosion process of fine sandy banks.
Lane et al (1994), Lindsay and Ashmore (2002) have also addressed the issue of survey frequency and its effect on underestimation of erosion volume due to unacounted erosion and deposition , which may occur within a single or on multiple flood events. However, bank surveying was not feasible during high flow events to investigate the mentioned process in detail.
Undercutting (in zone M) has induced almost no change in zone (IT), while it has caused intensive bank failure in zones (IIT) and (IIIT). Collapsed bank materials have been deposited on zone (IIB), while it has been eroded away in zone (IIIB). This process is the result of helical flow motion which reaches to its maximum strength in the zone (III) and induces intensive bank-toe erosion and transportation of eroded materials downstream.

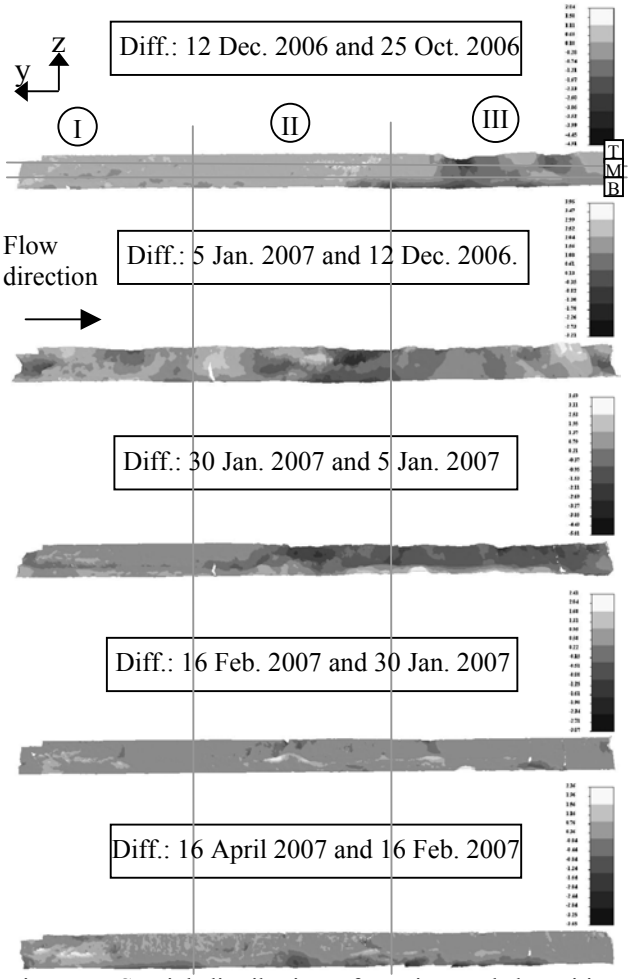

Figure 7. Spatial distribution of erosion and deposition along the riverbank in the rotated coordinate system within the bounded area. The erosion (-) and deposition (+) depths are in dm in x-direction (normal to the paper).

The most severe erosion volume of –0.564 m^3 has occurred during this period, with just a little amount of deposition (0.074m^3).
During the phase of decreasing flow, between 30 Jan. and 16 Feb. 2007 no significant bank surface changes occurred. Since the water level was under the bank-toe elevation. Although low water level still plays a role on bed erosion close to the bank. The computed net deposition

Table 2. Mean erosion (-) and deposition (+) depth (volume /surface) and net volume change along the outer riverbank.

row	Reference surface	Overlaying layer	Erosion depth(m)	deposition depth (m)	Net volume change(m^3)
1	2006.10.25	2006.12.12	-0.090	0.014	-0.274
2	2006.12.12	2007.01.05	-0.079	0.109	0.354
3	2007.01.05	2007.01.30	-0.153	0.049	-0.490
4	2007.01.30	2007.02.16	-0.016	0.014	0.014
5	2007.02.16	2007.04.16	-0.047	0.017	-0.107

of 0.014 m^3 confirms the negligible change in bank surface.

Two flood events with relatively long time interval and long duration occurred between 16 Feb. and 16 April 2007, which caused severe bank-toe erosion all along the zone (B) on the fluctuating area of water level, through which the bank height and bank-toe slope have increased.

An erosion volume of –0.143 m^3 was computed for this period, which shows less than one fourth of the erosion volume in the third study period, indicating the importance of peak flow amount and frequency on bank erosion in fine sandy soils.

The morphological processes involved in fine sandy riverbank erosion explained already along the river bend can be summarized as follows.

As it can be seen from representative cross sections from each aforementioned defined zones in figure 8, undercutting intensifies toward the downstream of the bend (cross sections II and III). This process triggers cantilever failure in the upper part of the riverbank at the two mentioned cross sections, while riverbank failure and undercutting are negligible processes at the beginning of the bend (cross section I).

The failed bank material are deposited on the bank-toe forming a berm at beginning and middle part of the bend (cross sections I and II), which decreases bank height and stabilizes the riverbank. On the other hand, failed bank materials are totally transported away at the downstream end of the bend (cross section III), as a result of intensifying helical flow motion in this zone, which causes increase of bank height and slope and destabilisation of the riverbank.

Bank-toe erosion is a process prevailing all along the river bend (in all three cross sections), causing increase of the bank height and slope of the berm-toe at section I and II and bank-toe in section III .

The second phase

In this phase the bank-toe processes has been studied. On 24 Oct. 2007, during low water stage period, the riverbank and bank-toe was scanned by laser scanner and the rest of the

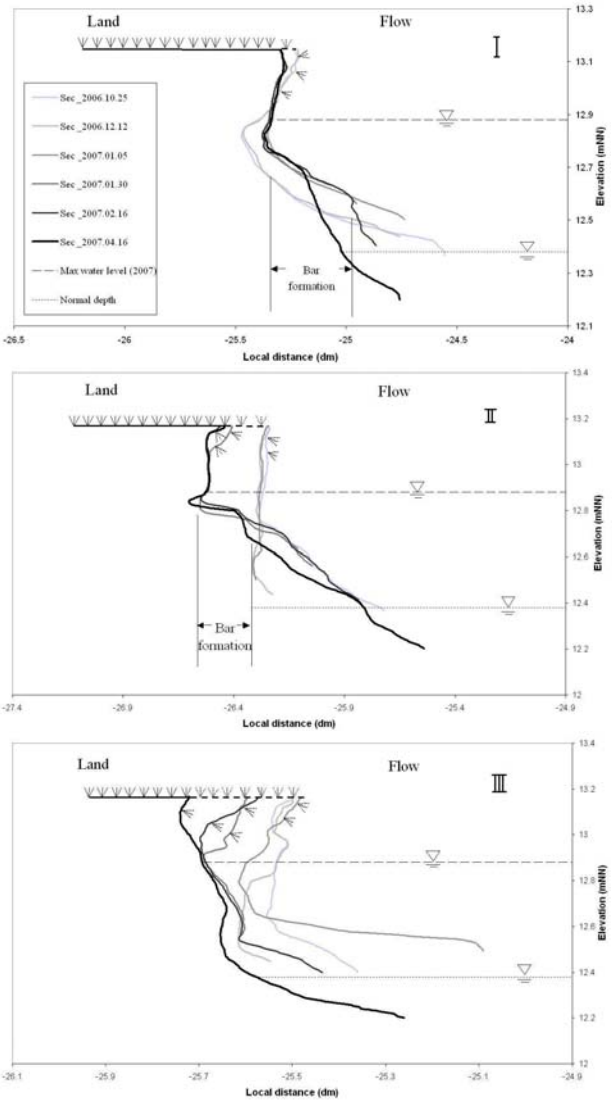

Figure 8.Representative cross sections in zones I to III.

river bed elevation was measured using echo-sounder and integrated to a single DTM model by the mentioned method in §3.3 .

As it is observed from the figure (9- b), failed bank material has formed a berm at bank-toe with decreasing berm width towards downstream. By subtracting the common area of this DTM surface from that of a bathymetry measurement on 20 July 2007 (figure9-a), it can be simply observed (figure 10-a) that between talweg and bank-toe, bars have been formed during this period due to the degradation of fine particles in low water stage and stabilisation by vegetation. The scour holes around berms get larger and deeper with the size of the berm.

Filtering echo-sounder noise data due to vegetation and low accuracy GPS data on 24

Oct. 2007 has affected the resolution of DTM model and made the talweg in the downstream part of bend seem to be flat, which has introduced positive bias in computed volume changes in table 3 .

Table 3. Mean erosion (-) and deposition (+) depth (volume /surface) and net volume change along the river bend.

row	Reference surface	Overlaying layer	Erosion depth(m)	deposition depth (m)	Net volume change(m^3)
1	2007.07.20	2007.10.24	-0.047	0.051	0.167
2	2007.10.24	2007.12.10	-0.081	0.129	1.266

a) 20 July 2007(with indication of section 1).

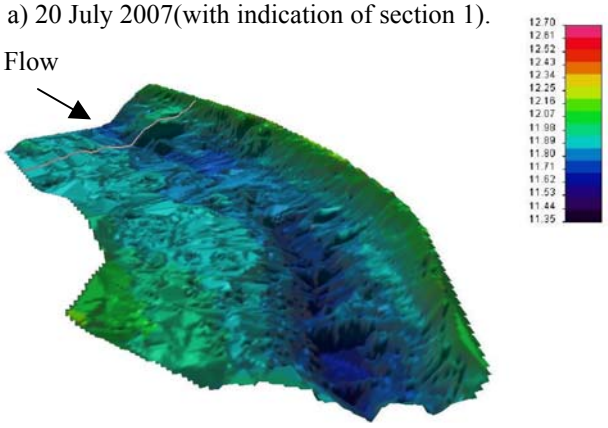

b) 24 Oct. 2007(with indication of section 2).

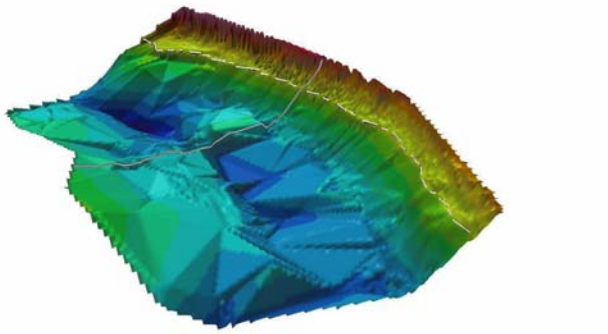

c) 10 Dec. 2007 (with indication of section 3).

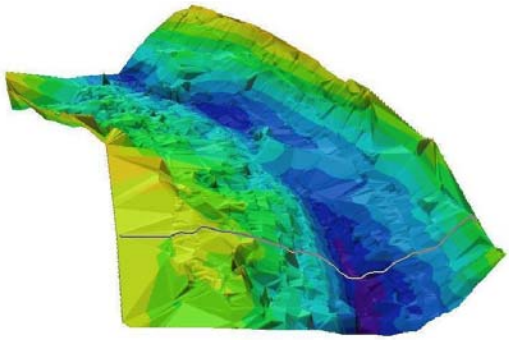

Figure 9. DTM models of the river bend using echo-sounder data, with vertical scale of two. In (b) the white dash line shows the imaginary border between echo-sounder and laser scanner data.

The erosion volume during mentioned period was -1.188 m^3. Net volume change in table 3 is the difference between erosion and deposition volumes.

During the high water stage on 10 Dec. 2007, the flow in river channel was almost bank full and laser scanner was not applicable. However, the whole bank-toe area was measured by echo-sounder. The talweg at downstream part of the bend has been extremely eroded destabilizing the riverbank around this zone (figure9-c) due to helical flow motion and secondary currents. This fact describes the reason of increasing bank failure amount towards downstream of the bend.

As it is seen in figure (10-b) most of the bank-toe area has faced erosion during this period and an appreciable amount of deposition has occurred on the inner side of the bend.

An erosion volume of 2.428 m^3 was computed for this period, while the deposition is about 3.694 m^3 .

a) Difference surface of 24 Oct. and 20 July 2007

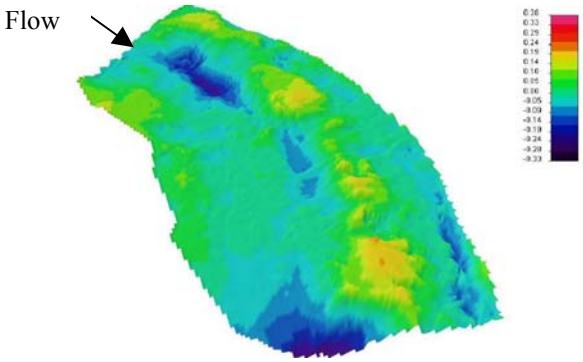

b) Difference surface of 10 Dec. and 24 Oct. 2007

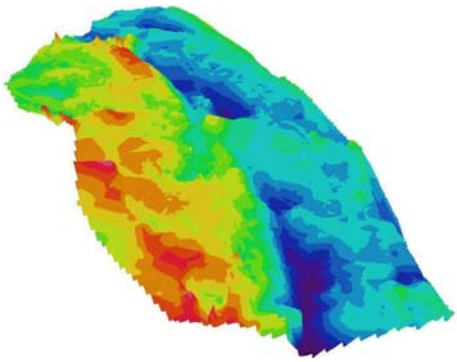

Figure 10. Bed erosion and deposition in the river bend in meter.

5 DISCUSSION

The distribution and amount of riverbank erosion and deposition zones along the river bend were computed by analysing the DTM models generated from terrestrial 3D laser scanner data and correlated with flood events with different flow peak frequencies and durations during the first study phase. It is observed that the shape of the flow hydrograph and frequency of peak flows play an important role in the riverbank and bank-toe erosion. The higher is the flood peak frequency and discharge, the more is the bank erosion in fine sandy rivers.

From the study of fluvial riverbank processes on both measurement phases, it can be concluded that in the beginning of the river bend, the failed bank material are mainly deposited at bank-toe as berm, while in the middle and exit zone of the river bend they are mainly eroded and transported to the inner side of the river bend and downstream by secondary flow currents. Therefore, bank height and slope are increased in the above-mentioned zones as two important factors in destabilizing of fine sandy slopes. And this is the reason of intensified riverbank erosion downstream part of the river bend(figure 9). However, the berm growth and erosion at the beginning of the river bend is dependent on the flow stage. Extreme flow events cause berm erosion even in the beginning of the river bend.

The dominant processes of fine sandy riverbank erosion can be explained referring to figure 11. Immediately after bank failure (figure 11-a), during a high flood event, the failed bank materials are deposited at bank-toe forming a berm. In subsequent flood events the riverbank is eroded by undercutting process (figure 11-b). Flow along the bank-toe, even in lower water stage, causes bank-toe erosion and combined by proceeding undercutting destabilizes the riverbank, which however remains stable due to matric suction in the riverbank during low water stages (figure 11-c). In the next high flood event, where pore pressure in the bank has been increased and matric suction has been already diminished, the overhanging part of the bank collapses due to its increased balk weight, caused by soil saturation, and deposits at bank-toe (except in the exiting end of the river bend, where intensive helical flow transports all the collapsed materials).

It is in contrast to Rinaldi and Casagli(1999) and Simon et al (2000), who believe that confining pressure of water in the river prevents bank failure in high water stages. This contradiction is due to absence of undercutting process in their bank failure model.

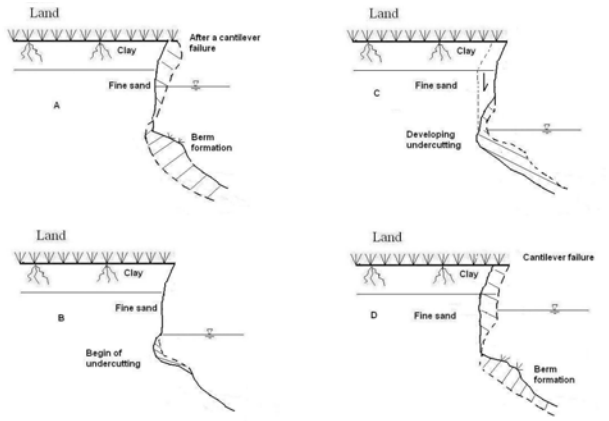

Figure 11. Description of fine sandy riverbank erosion. Dash line depicts the previous state. Dot line represents the probable next phase.

It can be then concluded that it is the flow situation with water level over river bank-toe elevation, which induces effective morphological changes on the riverbank surface in fine sandy banks. However low water stages play still an important role in berm- and bank-toe erosion.

It is noteworthy to point out the importance of a realistic wall shear stress modelling for simulation of fluvial erosion at bank-toe and undercutting process. Available 2D numerical models are capable of modelling 2D bed load transport models, however, fluvial processes taking place directly at bank surface, such as the mentioned ones, can only be modelled by 3D models with a realistic 3D wall shear stress model.

Overhang regions of the riverbank , vegetation zones of the river bed and GPS receipt quality are the most important factors affecting the accuracy of the applied techniques in the study.

6 CONCLUSION

A high resolution terrestrial 3D laser scanner was applied to study the morphological changes of a steep riverbank along the river bend. This technique offers higher accuracy and resolution, higher survey frequency and less cost than its airborne variant on small- and moderate-size reaches. The probability of unscanned zones due to shadowing effect of roughness elements and overhanging zones in this method is also minimized due to proximity to the target and the possibility of scanning from different angles and overlapping the scanning results.

The integration of terrestrial laser scanner data with echo-sounder data enabled the analysis of the river bathymetry in different water stages, in which one method was limited but the other was applicable.

There are different post-processing tools available for the analysis of huge amount of the laser scanner data, however for the special case of steep riverbanks with negative slopes, there is still a need for softwares capable of producing three-dimensional surfaces including folding zones and techniques for computation of their difference surfaces. The method of rotation of axis suggested here proved to be a simple solution to this shortcoming.

In fine sandy riverbanks, undercutting process together with bank-toe erosion play the key role in triggering cantilever bank failure and river bend migration.

7 ACKNOWLDGMENTS

The first author would like to acknowledge the German federal ministry of education and research for granting IPSWaT scholarship.

8 REFERENCES

Bitelli, G., Dubbini, M., and Zanutta, A. 2004. Terrestrial Laser Scanning and Digital Photogrammetry Techniques to Monitor Landslide Bodies, *10th ISPRS Congress*, Istanbul, Tukey,2004.

Brasington, J., Rumsby, B.T., and McVey, R.A. 2000. Monitoring and Modelling Morphological change in Braided Gravel-Bed River Using High-resolution GPS-based Survey. *Earth Surface Processes and Land Forms*, Vol. 25, 973-990

Entwistle, N.S., Heritage, G.L., Johnson , K., and Hetherington, D. 2007. Repeat Terrestrail Laser Scanner Survey of Bebble Cluster Creation and Formation in response to flow change, *, Annual Conference, Remote Sensing and Photogrammetry Society*, Newcastle,Upon Tyre,2007.

Fuller, I.C., Large, A.R.G., and Milan, D.J. 2003. Quantifying Development and Sediment Transfer Following Chute Cutoff in a Wandering Gravel-bed River. *Geomorphology,* Vol. 54. 307-232.

Heritage, G. and Hetherington, D. 2007. Towards a Protocol for Laser Scanning in Fluvial geomorphology, *Earth Surface Processes and Land Forms*, Vol. 32, 66-74.

Lane, S.N., Chandler J.H. and Richards, K.S. 1994. Developments in Monitoring and Modelling Small-Scale River Bed Topography, *Earth Surface Processes and Land Forms,* Vol.19, 349-368.

Large, A.R.G., and Heritage, G.L. 2007. Terrestrial Laser Scanner Based Instream Habitat Quantification Using a Random Field Approach*, Annual Conference, Remote Sensing and Photogrammetry Society*, Newcastle,Upon Tyre,2007.

Lawer, D.M. 1993.The Measurement of River Bank Erosion and Lateral Channel Change : A Review, *Earth Surface Processes and Land Forms*, Vol.18, 777-821.

Lindsay, J.B. and Ashmore P.E.2002. The Effects of Survey Frequency on Estimates of Scour and Fill in a Braided River Model, *Earth Surface Processes and Land Forms,* Vol. 27, 27-43.

Milan. D.J., Heritage, G.L.. and Hetherington, D. 2007. Application of a 3D Laser Scanner in the Assessment of Erosion and Deposition Volumes and Channel change in a Proglacial River, *Earth Surface Processes and Land Forms,* Vol.32, 1657-1674.

Mitasova, H., Drake, T., Harmon, R., Hofierka, J., and McNinch, J. 2002. Spatio-temporal Monitoring of Evolving Topography Using LiDAR, Real Time Kinematic GPS and Sonar Data. *Proceedings of the Open source GIS - GRASS users conference,* Trento, Italy, 2002.

Thoma, D.P., Gupta, S.C., and Bauer, M.A. 2001. Quantifying River Bank Erosion with Scanning Laser Altimetry*, International Archives of Photogrammetry and Remote Sensing*, Volume XXXIV-3/W4 Annapolis, MD., 2001,169-174.

Thoma, D.P., Gupta, S.C., and Bauer, M.A., Kirchoff, C.E. 2005. Airborne laser scanning for riverbank erosion assessment, *Remote Sensing of Environment*, Vol. 95, 493–501.

Rinaldi, M., Casagli, N. 1999. Stability of streambanks formed in partially saturated soils and effects of negative pore water pressures: the Sieve River(Italy), *Geomorphology*, Vol. 26, 253–277.

Simon, A., Curini, A., darby, S.E. and Langendoen, E.J. 2000. Bank and near-bank processes in an incised channel, *Geomorphology*, Vol. 35, 193–217.